

Journal of Biomedical Optics

SPIEDigitalLibrary.org/jbo

Investigation of nuclear nano-morphology marker as a biomarker for cancer risk assessment using a mouse model

Rajan K. Bista
Shikhar Uttam
Douglas J. Hartman
Wei Qiu
Jian Yu
Lin Zhang
Randall E. Brand
Yang Liu

Investigation of nuclear nano-morphology marker as a biomarker for cancer risk assessment using a mouse model

Rajan K. Bista,^a Shikhar Uttam,^a Douglas J. Hartman,^b Wei Qiu,^b Jian Yu,^b Lin Zhang,^c Randall E. Brand,^d and Yang Liu^a

^aUniversity of Pittsburgh, Department of Medicine and Bioengineering, Biomedical Optical Imaging Laboratory, Pittsburgh, Pennsylvania 15232

^bUniversity of Pittsburgh School of Medicine, Department of Pathology, Pittsburgh, Pennsylvania 15213

^cUniversity of Pittsburgh Cancer Institute, Department of Pharmacology and Chemical Biology, Pittsburgh, Pennsylvania 15213

^dUniversity of Pittsburgh, Department of Medicine, Division of Gastroenterology, Hepatology and Nutrition, Pittsburgh, Pennsylvania 15232

Abstract. The development of accurate and clinically applicable tools to assess cancer risk is essential to define candidates to undergo screening for early-stage cancers at a curable stage or provide a novel method to monitor chemoprevention treatments. With the use of our recently developed optical technology—spatial-domain low-coherence quantitative phase microscopy (SL-QPM), we have derived a novel optical biomarker characterized by structure-derived optical path length (OPL) properties from the cell nucleus on the standard histology and cytology specimens, which quantifies the nano-structural alterations within the cell nucleus at the nanoscale sensitivity, referred to as nano-morphology marker. The aim of this study is to evaluate the feasibility of the nuclear nano-morphology marker from histologically normal cells, extracted directly from the standard histology specimens, to detect early-stage carcinogenesis, assess cancer risk, and monitor the effect of chemopreventive treatment. We used a well-established mouse model of spontaneous carcinogenesis—*Apc*^{Min} mice, which develop multiple intestinal adenomas (Min) due to a germline mutation in the adenomatous polyposis coli (*Apc*) gene. We found that the nuclear nano-morphology marker quantified by OPL detects the development of carcinogenesis from histologically normal intestinal epithelial cells, even at an early pre-adenomatous stage (six weeks). It also exhibits a good temporal correlation with the small intestine that parallels the development of carcinogenesis and cancer risk. To further assess its ability to monitor the efficacy of chemopreventive agents, we used an established chemopreventive agent, sulindac. The nuclear nano-morphology marker is reversed toward normal after a prolonged treatment. Therefore, our proof-of-concept study establishes the feasibility of the SL-QPM derived nuclear nano-morphology marker OPL as a promising, simple and clinically applicable biomarker for cancer risk assessment and evaluation of chemopreventive treatment. © 2012 Society of Photo-Optical Instrumentation Engineers (SPIE). [DOI: 10.1117/1.JBO.17.6.066014]

Keywords: biomarker; phase microscopy; nano-morphology; optical path length; mouse model.

Paper 12021 received Jan. 10, 2012; revised manuscript received Apr. 16, 2012; accepted for publication Apr. 23, 2012; published online Jun. 4, 2012.

1 Introduction

Identification of effective biomarkers that can accurately predict cancer risk or serve as surrogates for preventive or therapeutic efficacy has become increasingly important, as more treatment options become available. However, the limited resource availability, high cost, and the inherent side-effects of many treatments preclude their use in all the affected individuals. Effective risk-assessment biomarkers can help to identify those individuals who are truly at highest risk of cancer, and also help in reducing the harm from overtreatment. Further, surrogate biomarkers for preventive or therapeutic efficacy represent potential intermediate endpoints for short-term intervention studies with preventive and therapeutic agents to measure the progress of treatment.

Carcinogenesis involves a complex series of molecular events that involve various distinct or interconnected pathways toward invasive cancer. Conventional pathology remains the gold-standard in cancer detection and various cell morphological characteristics often serve as predictors for cancer risk. However, they often have a limited accuracy in cancer risk

assessment, especially during the early-stage development of carcinogenesis. The conventional morphology only detects structural alterations at the micron scale, which are relatively insensitive to various molecular alterations associated with carcinogenesis. The recent advances in molecular technologies have identified a series of carcinogenesis-associated molecular biomarkers that may serve as more sensitive and reliable biomarkers for cancer risk assessment and detecting the early-stage carcinogenesis. Despite the great potential of these approaches, they can be confounded by intrinsic heterogeneity in tumorigenesis or multitude of separate molecular mechanisms underlying carcinogenesis.

While the micron-scale morphologic abnormalities may not be present early in the disease process, there are nanoscale molecular alterations in “normal” tissue early in the development of carcinogenesis. The nanoscale internal structural manifestations of various molecular events associated with carcinogenesis referred to as nano-morphology markers, have shown promise to serve as common shared characteristics for accurate cancer risk assessment despite the inherent heterogeneity.¹ The recent development in optical techniques has allowed the detection of these nanoscale structural properties.^{1–9} These changes occur at a scale of about 20 to 1000 times smaller than what conventional

Address all correspondence to: Yang Liu, University of Pittsburgh, Department of Medicine and Bioengineering, Biomedical Optical Imaging Laboratory, Department of Medicine and Bioengineering, University of Pittsburgh, Pittsburgh, Pennsylvania 15232.; Tel: 412-623-3751; Fax: 412-623-7828; E-mail: liuy@pitt.edu

optical microscope can detect. For example, partial-wave spectroscopy has shown that changes in the nano-structural properties could be highly sensitive for the detection of molecular alterations associated with carcinogenesis prior to the occurrence of phenotype.^{2,3,7,10,11} Moreover, other light scattering techniques have been employed to measure subcellular structure and provide noninvasive early detection of chemotherapy-induced apoptosis and to study calcium-induced alterations in mitochondrial morphology.^{12,13}

Our group has recently developed a novel optical microscope, Spatial-domain low-coherence quantitative phase microscopy (SL-QPM), that can detect subtle structural changes at sub-nanometer sensitivity, which is about 1000 times more sensitive than what conventional microscopy can detect.^{4-6,14} We derived nano-morphology markers quantified by nanoscale optical path length (OPL) properties from cell nuclei that showed a superior sensitivity in detecting carcinogenesis from histologically “normal” cells from cancer patients, suggesting that SL-QPM is a powerful tool to detect subtle nano-structural changes, not appreciated by conventional pathology.^{4,5} SL-QPM also has the advantage of being directly applicable on the standard histology and cytology specimens, and has the potential for clinical translation.

In the present study, we evaluate the feasibility of the nano-morphology markers extracted directly from standard tissue histology specimens as novel optical biomarkers for detecting early-stage carcinogenesis, assessing the cancer risk and evaluating the efficacy of chemopreventive agents. For this purpose, a well-established animal model—*Apc*^{Min} mouse model for carcinogenesis is used in this investigation. This animal model has *adenomatous polyposis coli* (*Apc*) gene mutation that causes spontaneous development of multiple intestinal neoplasia (Min),¹⁵ primarily in the small intestine. The mutations in the *Apc* tumor suppressor gene occur very early in the transformation process and are found in a majority of sporadic colorectal tumors as well as in the familial adenomatous polyposis.¹⁶ This model has previously been shown to be a robust indicator of tumorigenesis with changes in tumor number observed in response to a variety of preventive and therapeutic agents.¹⁷ Further, a well-documented chemopreventive agent—sulindac, a type of nonsteroidal anti-inflammatory drugs (NSAIDs) has been shown to be very effective in reducing the number and size of polyps and preventing colon cancer in human and rodent models.¹⁷⁻¹⁹ These characteristics make the *Apc*^{Min} mouse model an ideal system for our feasibility study. We first analyze the nano-morphology marker from the cell nuclei of normal epithelial cells in the small intestine at different stages of carcinogenesis to evaluate its ability to assess the cancer risk by its temporal correlations with future neoplasia. We then assess its ability to monitor the efficacy of chemopreventive agent sulindac by temporal correlations with the number and size of the tumors.

2 Materials and Methods

2.1 Animal Model

All animal studies were performed in accordance with the institutional Animal Care and Use Committee of the University of Pittsburgh. All mice were housed in micro isolator cages in a room illuminated from 7:00 AM to 7:00 PM (12:12-h light-dark cycle), with access to water and chow *ad libitum*. A total of 24 female mice were included in this study. A first set of three C57BL *Apc* wild-type mice and three age-

sex-matched C57BL *Apc*^{Min} mice were sacrificed at the age of six weeks. A second set of three C57BL *Apc* wild-type mice and three age-matched C57BL *Apc*^{Min} mice were sacrificed at the age of 4.5 months. Those *Apc*^{Min} mice at the age of six weeks had only a few microscopically-visible micro-adenomas; whereas those *Apc*^{Min} mice at the age of 4.5-month had developed visible multiple adenomatous polyps in their small intestine.

The small intestines tissue were removed, longitudinally opened and washed with phosphate buffered saline. A segment of small intestine (proximal and middle parts) was cut, and the individual slide from each animal was prepared following the standard tissue histology processing protocol with paraffin-embedding, sectioning at 4 μm thickness, mounting on a glass slide, paraffin removal and hematoxylin and eosin (H&E) staining. After staining, the tissue sections were covered with coverslips using mounting media.

2.2 Chemopreventive Study

Two groups of ten-week-old sex-matched *Apc*^{Min} mice comprising of six mice in each group were fed with control or experimental high-fat AIN93G diet (Dyets) containing 200 ppm (approximately 20 mg/kg/d) of sulindac (Sigma) for two weeks and four months as previously described.^{17,18} Mice were sacrificed immediately after the treatment. The number of tumors was counted under the dissection microscope (polyps; >0.5 mm in diameter). Afterwards, a segment of small intestine was cut and then prepared into “Swiss-rolls” and processed following standard histology protocol as mentioned earlier.

2.3 Analysis of the Nuclear Nano-Morphology Marker from Cell Nucleus

The nano-morphology marker from the cell nucleus is derived using a recently developed optical microscopy system—SL-QPM. The technical development of SL-QPM system has been described in detail in our previous publications.^{4,5,20} We obtain an OPL map of the individual cell nucleus under observation, which is sensitive to subtle structural changes in the cell nucleus with nanoscale sensitivity.

In brief, SL-QPM system uses reflection-mode common-path interferometer configuration combined with a low-coherence light source and spectroscopic detection and records a three-dimensional spectroscopic intensity data cube [$I(x, y, z)$; k = free-space wavenumber, (x, y) corresponds to the specific pixel of the image], predominately the interference signals between the backscattered reference wave and the backscattered sample wave. These interference signals were mathematically transformed via the pixel-wise Fourier transform of $I(x, y, z)$ along the k direction—after removing the bias term—gives us $I_F(x, y, z')$, where z' is the OPL. The $I_F(x, y, z')$ is then used to find the prominent peak corresponding to the OPL of interest, z_p . We then calculate the structure-derived OPL with the equation $\text{OPL}(x, y) = z_p + \angle I(x, y, z')|_{z'=z_p} / (2k)$, where $\angle I(x, y, z')$ represents the phase term and the factor 2 in the denominator of above relation accounts for the double path length geometry due to the reflectance-mode configuration and the free-space wavenumber k corresponds to $\lambda_0 = 550$ nm. The nanoscale structural sensitivity comes from the second term of this equation. Figure 1 illustrates the data processing steps of this system. We also account for the effect of variation in the stain-induced structure-derived OPL using a staining correction

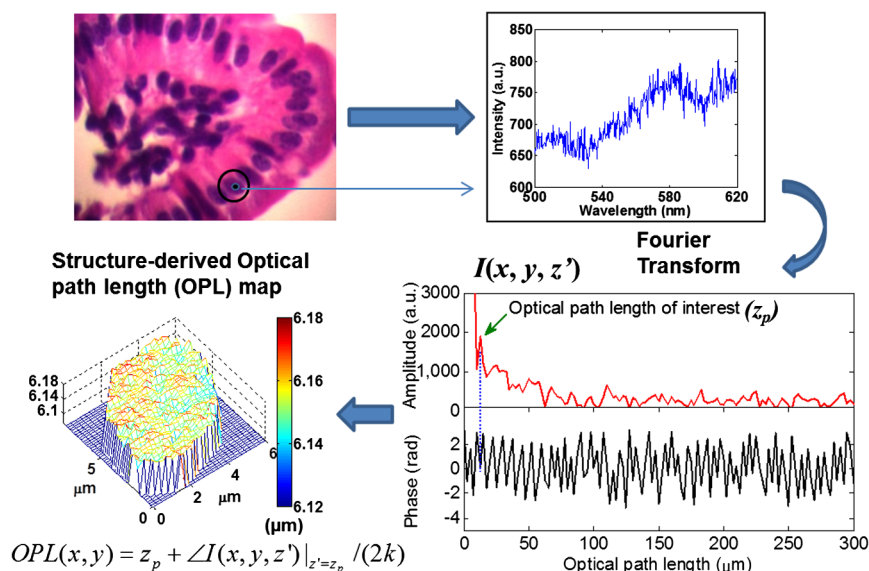


Fig. 1 Schematics of the data processing steps involved in the spatial-domain low-coherence quantitative phase microscopy (SL-QPM) system.

model.²⁰ As a result, the structure-derived OPL map can be obtained from each cell nucleus.

2.4 Statistical Analysis

To quantify the statistical nano-morphology characteristics of the structure-derived OPL map in the nucleus, we extracted the average $\langle OPL \rangle$ from each cell nucleus as the representative statistical nuclear nano-morphology marker. We analyzed this marker for approximately 50 to 60 epithelial cell nuclei from each sample. To minimize the variations of cell appearance due to tissue sectioning, we particularly focused on the columnar-shaped epithelial cells having similar morphological features such as intact nuclear boundary and no overlap of nucleus as marked region in Fig. 2. The statistical analysis was performed using the student's t-test (Microsoft Excel 2010). Two-sided P values (assuming unequal variances) were used for all analyses. A two-sided P value of 0.05 or less was considered as statistically significant.

3 Results

We first examined whether the nuclear nano-morphology marker deduced from the structure-derived OPL can be used to predict the concurrent and future neoplasm in the well-established animal model of colorectal carcinogenesis— Apc^{Min} mice. In this mouse model, the majority of the intestinal adenomatous polyps occur in the small intestine and tumors occur in a well-established chronology. The mice at six weeks represent an early-stage carcinogenesis without any visible tumors and with only microscopically visible micro-adenomas; while those at 4.5 months represent an advanced stage of carcinogenesis with multiple macroscopically visible adenomatous polyps (tumors).

3.1 Structure-Derived Optical Path Length (OPL) Map from Cell Nuclei Detects the Concurrent and Future Neoplasm from Normal Intestinal Epithelial Cells

We first analyzed the histologically normal epithelial cells from the small intestine from two sets of age-matched wild-type mice and Apc^{Min} mice at six weeks and 4.5 months. Figure 2 shows

the representative conventional bright-field images and corresponding structure-derived nuclear OPL maps for three selected nuclei of the histologically normal intestinal epithelial cells for (a) a six-week wild-type mouse, (b) a six-week Apc^{Min} mouse, and (c) a 4.5-month Apc^{Min} mouse. Although these cells are labeled as “normal” by an expert pathologist (DJH), their pseudo-color nuclear OPL maps exhibit a progressive change. The pre-dominant blue color from the cell nucleus of the wild-type mouse suggests a smaller value of OPL, compared to the nuclear OPL map from the six-week and 4.5-month mice, suggesting the promise of using nuclear structural abnormalities to detect the subtle structural changes that are not appreciated by using conventional pathology approach.

3.2 Statistical Analysis of Nuclear Nano-Morphology Marker from the Cell Nucleus

Based on the above structure-derived nuclear OPL maps of histologically normal cells, we performed the statistical analysis for ~ 50 to 60 epithelial cell nuclei for each mouse. As shown in Fig. 3, the nuclear nano-morphology marker of $\langle OPL \rangle$ from histologically normal epithelial cells (i.e., uninvolved cells) from small intestine show a progressive increase from wild-type mice, to six-week mice, to 4.5-month mice ($P = 0.01$ between six weeks and 4.5 months), which parallels the development of colon carcinogenesis. Importantly, there is a statistical significance even for early-stage neoplastic changes of six weeks in Apc^{Min} mice ($P = 0.001$) and follows the temporal progression of intestinal tumorigenesis with more elevated value of nuclear $\langle OPL \rangle$ in the advanced neoplastic stage of 4.5 months ($P = 8.1E - 11$), suggesting that this nuclear nano-morphology marker detects the subtle structural changes beyond the morphologically evident tumor (i.e., the histologically normal cells from Apc^{Min} mice). It is a good indicator to predict a genetic substrate to neoplastic transformation before occurrence of neoplasia. We also found that the values of nuclear $\langle OPL \rangle$ for the wild-type mice at different ages of six weeks and 4.5 months are not statistically significant ($P = 0.1$), suggesting that the nano-morphology markers do not appear to be compromised by confounding factors contributed by the age of the mice.²¹

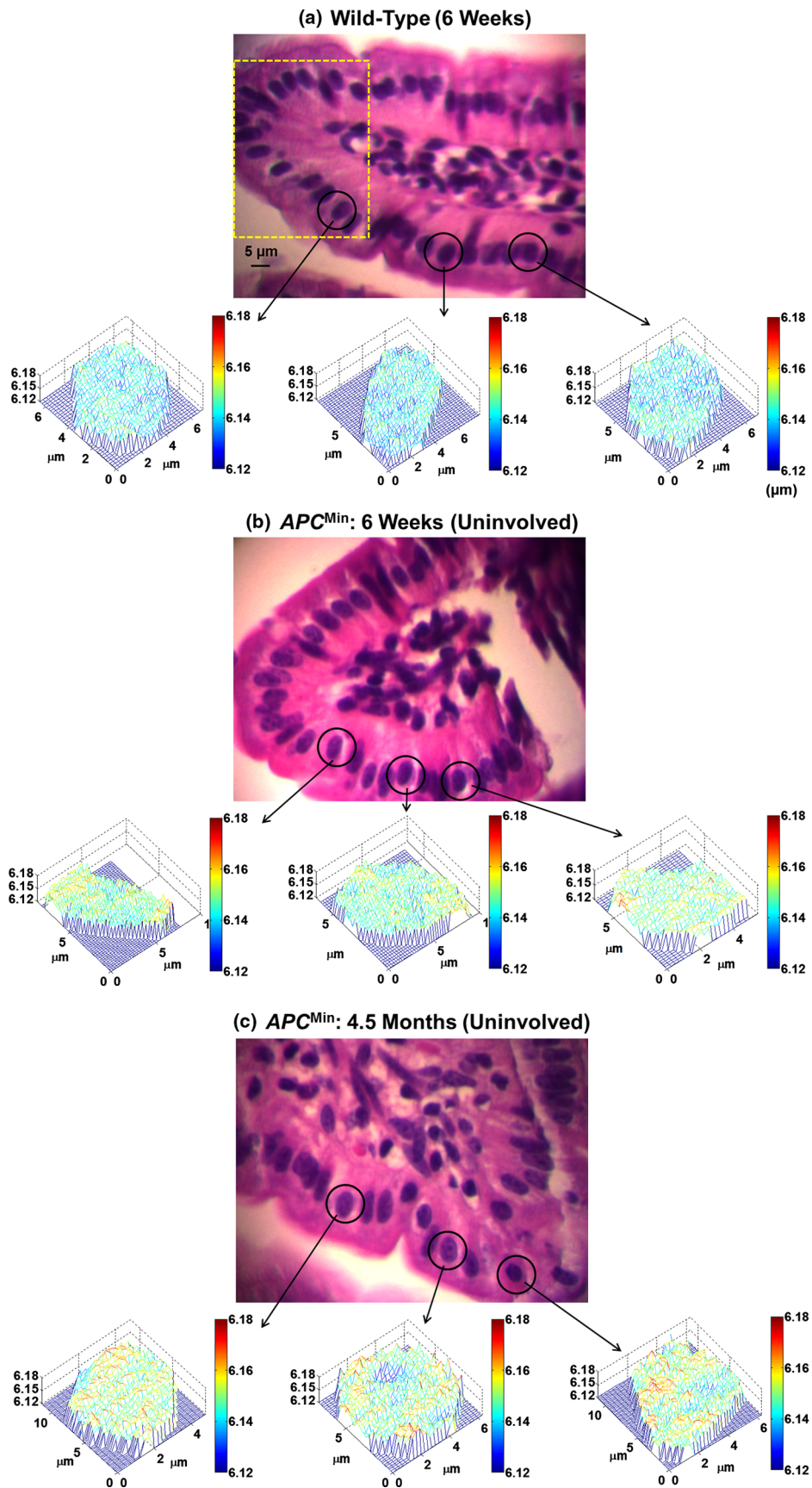


Fig. 2 Representative regular bright-field images of H&E stained epithelial cell nuclei and corresponding structure-derived nuclear optical path length (OPL) maps for three selected cells derived from (a) wild-type mouse (six weeks), (b) histologically normal appearing cells (uninvolved cells) from six weeks APC^{Min} mouse, and (c) histologically normal appearing cells (uninvolved cells) from 4.5 months APC^{Min} mouse. The marked area in part (a) shows the representative columnar shaped epithelial cells having similar morphological features.

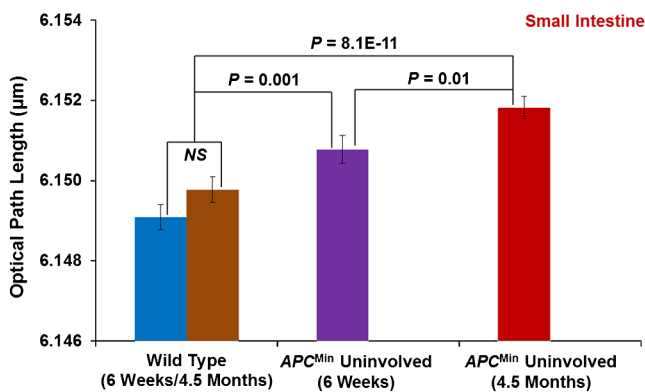


Fig. 3 Statistical analysis of the nuclear nano-morphology marker characterized by structure-derived optical path length (OPL) from the cell nuclei of wild-type mice and histologically normal (i.e., uninvolved) appearing intestinal epithelial cell nuclei from gender and age-matched *Apc^{Min}* mice at six weeks and 4.5 months. The nuclear OPL exhibits a progressive increase with the development of carcinogenesis. Approximately 50 to 60 cell nuclei were analyzed from each mouse.

3.3 Performance of Nuclear Nano-Morphology Markers

The scatter plots in Fig. 4 present the cell-to-cell variation of nano-morphology markers [$\langle OPL \rangle$ and the intra-nuclear standard deviation of OPL (σ_{OPL})] in the wild-type and *Apc^{Min}* mice at six weeks and 4.5 months. Despite the intrinsic variation, these histologically normal cells from the *Apc^{Min}* mice occupy a distinct region with minor overlap compared to those from the wild-type mice. However, such cell-to-cell variation within the same animal is much smaller than the inter-group animal variation (wild-type versus *Apc^{Min}* group), as quantified by the *p*-values ($P < 0.05$) presented in the previous section.

Further, to use these nuclear nano-morphology markers for future clinical use to assess the risk of developing carcinogenesis for each patient, we have to obtain the patient-based characteristic statistical measure. In this proof-of-concept study with the animal model, the average values of $\langle OPL \rangle$ and the intra-nuclear standard deviation of OPL (σ_{OPL}) denoted respectively as $\langle OPL \rangle_m$ and $\langle \sigma_{OPL} \rangle_m$, were taken from about 50 to 60 cell nuclei as characteristic subject-specific marker for each mouse. Figure 5 shows the scatter plot of $\langle OPL \rangle_m$ and $\langle \sigma_{OPL} \rangle_m$ for each mouse at different time points. It is evident that there is a clear separation between the wild-type mice and *Apc^{Min}* mice group, as indicated by the solid line in Fig. 5. All of those mice with the risk of developing carcinogenesis (even those at the early stage) are detected by the nuclear nano-morphology markers.

3.4 Chemoprevention Studies with Sulindac

To further confirm the neoplastic relevance of the nuclear nano-morphology marker quantified by OPL and evaluate its potential to monitor the efficacy of preventive agents, we investigated how the nuclear nano-morphology marker from histologically normal cells changes as a response to the treatment using an established chemopreventive agent, sulindac. It has been previously shown that dietary supplementation with NSAIDs such as sulindac for several months prevent adenoma formation in the small intestine of *Apc^{Min}* mice.²² We showed that sulindac has significantly reduced number of polyps after four-month treatment in the *Apc^{Min}* mice, as shown in Fig. 6. The 4-month

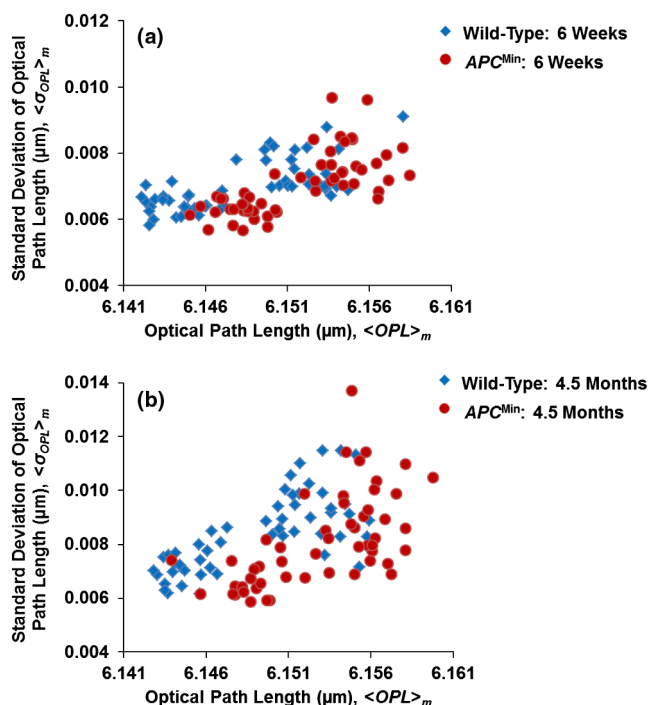


Fig. 4 The scatter plots showing the cell-to-cell variation from the histologically normal cells from wild-type and *Apc^{Min}* mice at (a) six weeks and (b) 4.5 months. Despite the intrinsic variation, the histologically normal cells from the *Apc^{Min}* mice occupy a distinct regime compared to those from wild-type mice.

sulindac treatment prevents intestinal tumors by reducing the number of polyps (≥ 0.5 mm in diameter) by $\sim 88\%$ (from approximately 85 in untreated mice to 10 after 4-month treatment, $P < 0.0001$).¹⁷

Figure 7 demonstrates the statistical analysis of the structure-derived nuclear $\langle OPL \rangle$ from histologically normal intestinal epithelial cells of untreated *Apc^{Min}* mice and sulindac-treated *Apc^{Min}* mice for two weeks and four months treatment. For

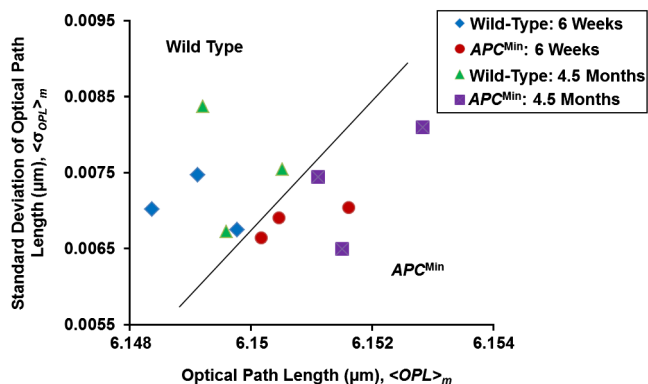


Fig. 5 The scatter plot of the individual-animal based characteristic nano-morphology markers characterized by the mean values ($\langle OPL \rangle_m$ and $\langle \sigma_{OPL} \rangle_m$) of intra-nuclear (OPL) and intra-nuclear standard deviation of optical path length σ_{OPL} averaged over 50 to 60 cell nuclei for each wild-type and *Apc^{Min}* mouse. Evidently, the nuclear nano-morphology markers can clearly distinguish wild-type mice from *Apc^{Min}* mice (even at the early-stage carcinogenesis), as indicated by the solid line.

untreated Apc^{Min} mice, the nuclear ⟨OPL⟩ in the histologically normal intestinal epithelial cells significantly increases with time ($P = 1.0E - 5$); while for sulindac-treated Apc^{Min} mice, the values of nuclear ⟨OPL⟩ in the normal intestinal epithelial cells do not show a statistically significant increase over time at six weeks and four months ($P = 0.3$). At the early-stage of the sulindac treatment (two weeks), the normal intestinal epithelial cells show a slight decrease of nuclear ⟨OPL⟩ ($P = 0.4$, no statistical significance) in the Apc^{Min} mice compared to the untreated mice. But after four months of prolonged treatment with sulindac, their nuclear ⟨OPL⟩ value significantly decreases, compared to those untreated Apc^{Min} mice ($P = 4.7E - 5$), and reversed to normal. These results are consistent with the finding that the number of tumors has significantly reduced after the prolonged treatment of sulindac. These data also further confirm that the nuclear nano-morphology marker defined by OPL from the histologically normal intestinal epithelial cells is truly due to the neoplastic changes, rather than other nonspecific changes in the animal model. The result also shows a potential of using the nuclear OPL as a surrogate marker to monitor the effect of chemopreventive treatment.

4 Discussion

With the use of a well-established animal model of colon carcinogenesis and chemo-preventive agent, we report herein the significant alteration of the nano-morphology marker characterized by structure-derived OPL from the cell nuclei in the histologically normal intestinal epithelial cells that precede the development of the phenotype (i.e., adenomas). The progressive change in this nano-morphology marker parallels the progression of carcinogenesis. Further, this marker is reversed to normal as a response to the treatment of the potent chemopreventive agent sulindac. Hence, such nano-morphology marker represents a powerful means of detecting an inherited cancer risk, monitoring the progression of carcinogenesis even at the early stage, and for evaluation of response to chemoprevention.



Fig. 6 Longitudinally opened sections of small intestine; (a) Apc^{Min} /untreated mice and (b) Apc^{Min} /sulindac treated mice. Sulindac significantly reduced the number of polyps after 4-month treatment.

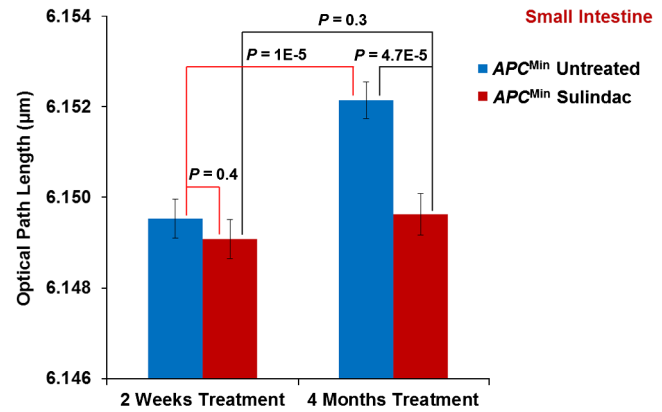


Fig. 7 Statistical analysis of the nuclear optical path length (OPL) from the nuclei of intestinal epithelial cells in the Apc^{Min} mice with regular diet and with sulindac supplement. The progression of nuclear OPL in the histologically normal (i.e., uninvolved) intestinal epithelial cell nuclei significantly slowed down after 4-month of sulindac treatment ($P = 0.3$) compared to the corresponding untreated Apc^{Min} mice ($P = 1E - 5$). The nuclear OPL from sulindac-treated mice is significantly lower than those untreated Apc^{Min} mice ($P = 4.7E - 5$). Approximately 50 to 60 cell nuclei were analyzed from each mouse.

The nuclear nano-morphology marker is derived from a recently developed novel optical microscope—spatial-domain low-coherence quantitative phase microscopy (SL-QPM). It represents a novel class of cellular characteristics for evaluating nanoscale structural changes in the cell nucleus that could accompany the complex accumulation of molecular alterations during carcinogenesis. SL-QPM takes advantage of the ultra-high sensitivity of the light interference effect to achieve nanoscale sensitivity not attainable with a conventional microscope.^{4,5} Compared with other biomarkers, the nano-morphology marker has a few major advantages. First, it can be extracted from the clinical tissue histology specimens (glass-slide-based) prepared according to standard routine clinical protocols without any additional processing, thus easily can be integrated with the existing workflow of current pathology laboratories. Second, the analysis of nuclear nano-morphology marker does not require any consumable agents, so there is no additional cost or effort in preparing the sample.

The nuclear nano-morphology marker shows the ability to detect the presence of “field effect” in carcinogenesis, or detect the presence of neoplastic conditions from histologically normal cells adjacent to or distant from the tumor. For example, for those cells labeled as “normal” by the expert gastrointestinal pathologist, their nuclear OPL are significantly elevated in the Apc^{Min} mice at both early-stage of carcinogenesis of six weeks without development of any visible tumors and an advanced neoplastic stage of 4.5 months with multiple adenomatous polyps, when compared to those from the wild-type mice. The field effect in the Apc^{Min} mice results from the genetic predisposition to the development of carcinogenesis.²³ Besides the inherited genetic defects, other significant biochemical and genetic molecular abnormalities have also been reported to contribute to the altered “cancer field” in the histologically normal intestinal mucosa of the Apc^{Min} mice, such as altered β -catenin,²⁴ cell proliferation, apoptosis,²⁵ and metabolic alterations.²⁶ Although the specific biological mechanisms responsible for the detected changes in nuclear OPL are still unknown, the reported biological processes provide the biological plausibility. One or more of the molecular, cellular and biochemical

events associated with “field effect” may also be responsible for the change in the nuclear nano-morphology marker OPL. For example, our recent finding revealed that increased DNA content is one of the contributing factors for the increased nuclear OPL observed in carcinogenesis.¹⁴

The detection of such “field effect” can also be used as an early-stage marker to monitor the progression of carcinogenesis and predict the future neoplastic risk, as suggested by the temporal correlation of the nano-morphology marker of nuclear OPL with the neoplastic progression. The most significant progression ($P = 0.001$) occurs between the wild-type mice and the *Apc*^{Min} mice at the pre-adenomatous stage (six weeks), well preceding the development of visible tumor (i.e., adenomatous polyps). The neoplastic relevance of nuclear OPL is further underscored by its significant reversal to normal (wild-type) mice, as a response to sulindac treatment that leads to a significant reduction (~88%) in the number of tumors. This result suggests that the nano-morphology marker of the histologically normal epithelial cells detects the tumor-suppressing ability of chemopreventive agents and can also serve as an early-stage surrogate marker to monitor the efficiency of chemopreventive agents.

In conclusion, in this proof-of-concept study using a well-established animal model of carcinogenesis—*Apc*^{Min} mouse model and an efficient chemopreventive agent of sulindac, we evaluated the use of a novel nuclear nano-morphology marker quantified by structure-derived OPL, extracted directly from standard histology specimens, as a potential biomarker to detect the early-stage carcinogenesis, assess the cancer risk and monitor the efficiency of chemopreventive agents. We demonstrated that the nuclear nano-morphology marker OPL detects the presence of neoplasm from histologically normal cells, or cancer “field effect.” The temporal correlation of the nuclear nano-morphology marker OPL with the neoplastic progression suggests its use as an early-stage biomarker to predict the future neoplastic risk. Moreover, the substantial reversal of this biomarker to normal as a response to the chemopreventive agent of sulindac suggests its use as a surrogate marker to gauge the chemopreventive efficacy for cancer risk reduction. This marker is currently being evaluated for identifying patients who are at an increased risk of developing malignancy and as a surrogate marker for monitoring the effect of chemopreventive agents. If proven successful in clinical studies, it will help in identifying patients with truly high-risk for proper preventive or therapeutic treatment. This nano-morphology marker is derived from the standard tissue histology specimens, and therefore could be readily translated to clinical settings.

Acknowledgments

We gratefully acknowledge the National Institute of Health (R21CA152935), American Cancer Society (RGS-10-124-01-CCE), Wallace H. Coulter foundation and University of Pittsburgh Medical Center for supporting this research. The authors appreciate the help from Kevin Staton in sample preparation.

References

- H. K. Roy, T. Hensing, and V. Backman, “Nanocytology for field carcinogenesis detection: novel paradigm for lung cancer risk stratification,” *Future Oncol.* **7**(1), 1–3 (2011).
- H. Subramanian et al., “Optical methodology for detecting histologically unapparent nanoscale consequences of genetic alterations in biological cells,” *Proc. Natl. Acad. Sci. USA* **105**(51), 20118–20123 (2008).
- H. Subramanian et al., “Nanoscale cellular changes in field carcinogenesis detected by partial wave spectroscopy,” *Cancer Res.* **69**(13), 5357–5363 (2009).
- P. Wang et al., “Spatial-domain low-coherence quantitative phase microscopy for cancer diagnosis,” *Opt. Lett.* **35**(17), 2840–2842 (2010).
- P. Wang et al., “Nanoscale nuclear architecture for cancer diagnosis beyond pathology via spatial-domain low-coherence quantitative phase microscopy,” *J. Biomed. Opt.* **15**(16), 066028 (2010).
- P. Wang et al., “An insight into statistical refractive index properties of cell internal structure via low-coherence statistical amplitude microscopy,” *Opt. Express* **18**(21), 21950–21958 (2010).
- N. T. Shaked et al., “Quantitative phase microscopy of articular chondrocyte dynamics by wide-field digital interferometry,” *J. Biomed. Opt.* **15**(1), 010505 (2010).
- I. Itzkan et al., “Confocal light absorption and scattering spectroscopic microscopy monitors organelles in live cells with no exogenous labels,” *Proc. Natl. Acad. Sci. USA* **104**(44), 17255–17260 (2007).
- B. Kemper et al., “Integral refractive index determination of living suspension cells by multifocus digital holographic phase contrast microscopy,” *J. Biomed. Opt.* **12**(5), 054009 (2007).
- H. K. Roy et al., “Optical detection of buccal epithelial nanoarchitectural alterations in patients harboring lung cancer: implications for screening,” *Cancer Res.* **70**(20), 7748–7754 (2010).
- R. K. Bista et al., “Using optical markers of nondysplastic rectal epithelial cells to identify patients with ulcerative colitis-associated neoplasia,” *Inflamm. Bowel Dis.* **17**(12), 2427–2435 (2011).
- K. J. Chalut et al., “Light scattering measurements of subcellular structure provide noninvasive early detection of chemotherapy-induced apoptosis,” *Cancer Res.* **69**(3), 1199–1204 (2009).
- N. N. Boustany, R. Drezek, and N. V. Thakor, “Calcium-induced alterations in mitochondrial morphology quantified in situ with optical scatter imaging,” *Biophys. J.* **83**(3), 1691–1700 (2002).
- R. K. Bista et al., “Quantification of nanoscale nuclear refractive index changes during the cell cycle,” *J. Biomed. Opt.* **16**(7), 070503 (2011).
- K. W. Kinzler and B. Vogelstein, “Lessons from hereditary colorectal cancer,” *Cell* **87**(2), 159–170 (1996).
- B. Vogelstein and K. W. Kinzler, “Cancer genes and the pathways they control,” *Nat. Med.* **10**(8), 789–799 (2004).
- W. Qiu et al., “Chemoprevention by nonsteroidal anti-inflammatory drugs eliminates oncogenic intestinal stem cells via SMAC-dependent apoptosis,” *Proc. Natl. Acad. Sci. USA* **107**(46), 20027–20032 (2010).
- W. Qiu et al., “PUMA suppresses intestinal tumorigenesis in mice,” *Cancer Res.* **69**(12), 4999–5006 (2009).
- S. J. Shiff et al., “Sulindac sulfide, an aspirin-like compound, inhibits proliferation, causes cell cycle quiescence, and induces apoptosis in HT-29 colon adenocarcinoma cells,” *J. Clin. Invest.* **96**(1), 491–503 (1995).
- S. Uttam et al., “Correction of stain variations in nuclear refractive index of clinical histology specimens,” *J. Biomed. Opt.* **16**(11), 116013 (2011).
- L. L. Shen et al., “MGMT promoter methylation and field defect in sporadic colorectal cancer,” *J. Natl. Cancer Inst.* **97**(18), 1330–1338 (2005).
- Y. Beazer-Barclay et al., “Sulindac suppresses tumorigenesis in the Min mouse,” *Carcinogenesis* **17**(8), 1757–1760 (1996).
- B. J. Braakhuis et al., “A genetic explanation of Slaughter’s concept of field cancerization: evidence and clinical implications,” *Cancer Res.* **63**(8), 1727–1730 (2003).
- K. Aoki and M. M. Taketo, “Adenomatous polyposis coli (APC): a multi-functional tumor suppressor gene,” *J. Cell Sci.* **120**(19), 3327–3335 (2007).
- S. V. Russello and S. K. Shore, “SRC in human carcinogenesis,” *Front Biosci: A J Virtual Library* **9**, 139–144 (2004).
- A. Backshall et al., “Detection of metabolic alterations in non-tumor gastrointestinal tissue of the *Apc*(Min/+) mouse by (1)H MAS NMR spectroscopy,” *J. Proteome Res.* **8**(3), 1423–1430 (2009).